

## Intrinsic Emittance Reduction of an Electron Beam from Metal Photocathodes

C. P. Hauri, R. Ganter, F. Le Pimpec, A. Trisorio, C. Ruchert, and H. H. Braun

*Paul Scherrer Institute, 5232 Villigen, Switzerland*

(Received 1 April 2010; published 10 June 2010)

Electron beams in modern linear accelerators are now becoming limited in brightness by the intrinsic emittance of the photocathode electron source. Therefore it becomes important for large scale facilities such as free electron lasers to reduce this fundamental limit. In this Letter we present measurements of the intrinsic emittance for different laser wavelength (from 261 to 282 nm) and for different photocathode materials such as Mo, Nb, Al, Cu. Values as low as  $0.41 \pm 0.03$  mm · mrad/mm laser spot size (rms) were measured for a copper photocathode illuminated with a 282 nm laser wavelength. The key element for emittance reduction is a uv laser system which allows adjustment of the laser photon energy to match the effective work function of the cathode material and to emit photoelectrons with a lower initial kinetic energy. The quantum efficiency over the explored wavelength range varies by less than a factor of 3.

DOI: 10.1103/PhysRevLett.104.234802

PACS numbers: 29.25.Bx, 41.60.Cr, 52.59.Wd, 85.60.Ha

Modern linear accelerators very efficiently preserve the electron beam emittance throughout acceleration. In consequence, it becomes important to extract electrons from a cathode with the lowest possible emittance. rf photocathode guns have shown their capability for high-brightness electron beam generation with a transverse emittance mostly limited by the intrinsic emittance [1,2]. The intrinsic emittance is the lowest possible limit for a given cathode material, surface electric field, and laser wavelength. Several free electron laser (FEL) facilities have reported measurements of intrinsic emittance which were significantly larger than what is expected from theory [1,2].

In the framework of the SwissFEL project at Paul Scherrer Institute [3,4], an electron gun test facility [5] has been built in order to study new schemes for reducing electron beam emittance from the source. Reduction of the intrinsic emittance by tuning the laser wavelength illuminating the cathode is the scheme explored in this Letter. An important difference to previously published intrinsic emittance measurements is the extremely low electron beam charge used in our work ( $< 1$  pC). This allows for accurate determination of intrinsic emittance due to the elimination of space-charge induced emittance degradation. All the emittance measurements were done at 6 MeV in a pulsed diode gun with an rf booster cavity [5]. The measured emittance values are in good agreement with the theoretical values of intrinsic emittance for metallic photocathodes [6]. The systematic studies presented here on wavelength-dependent emittance have become possible due to the development of a high-power uv laser with a tunable central wavelength [7].

Neglecting intrinsic effects ( $T = 0$ ) the intrinsic emittance at the surface of a cathode can be expressed analytically as [6]

$$\varepsilon_{\text{intr}} = \sigma_r \sqrt{\frac{\hbar\omega - (\Phi_0 - \sqrt{e^3 F / 4\pi\epsilon_0})}{3mc^2}} \quad (1)$$

with  $\sigma_r$  the laser spot size (rms),  $\hbar\omega$  the laser photon energy,  $\Phi_0$  the work function of the cathode material,  $F$  the effective surface electric field,  $T$  the cathode temperature,  $mc^2$  and  $e$  the electron rest mass energy and charge, respectively. Equation (1) suggests two ways to reduce the intrinsic emittance  $\varepsilon_{\text{intr}}$  at the cathode surface: by reducing emitting area size  $\sigma_r$ , or by matching the photon energy  $\hbar\omega$  to the effective work function  $\Phi_{\text{eff}}$ . The effective work function  $\Phi_{\text{eff}}$  is the material work function lowered by the Schottky term [ $\Phi_{\text{eff}} = \Phi_0 - (e^3 F / 4\pi\epsilon_0)^{1/2}$ ]. The Schottky term corresponds to the potential barrier reduction due to the applied electric field. A detailed description of the intrinsic emittance theory for metallic photocathodes can be found elsewhere [6,8]. With the wavelength-tunable laser source it becomes possible to vary the energy of the photons in order to match the potential barrier height modified by the Schottky effect. A drop in quantum efficiency (QE) is expected when one approaches the limit where the photon energy compensate the effective work function [9]. In this Letter simultaneous measurements of emittance and QE when varying the laser wavelength have been performed for different photocathode materials such as Mo, Nb, Al, and Cu.

The accelerator beam line used for this study (Fig. 1) consists of an electron gun in a diode configuration followed by a two-cell rf cavity ( $f_{\text{rf}} = 1.5$  GHz). The distance cathode to anode is 6 mm and negative voltage pulses

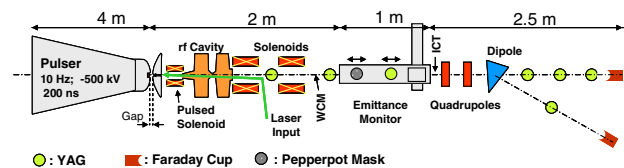


FIG. 1 (color online). SwissFEL electron gun test stand. WCM: wall current monitor, ICT: integrating current transformer.

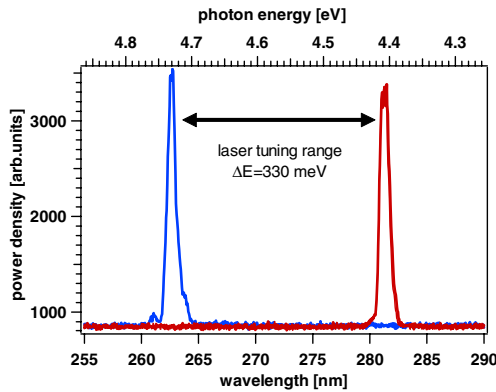


FIG. 2 (color online). Spectral tuning range of uv laser covering photon energies of 4.4 to 4.73 eV.

of 300 kV amplitude and 200 ns full width half maximum (FWHM) duration are applied to the diode. The metallic photocathode is inserted in a so-called hollow geometry (inset is recessed in regard to the holding lips [5]) so that the electric field gradient on the cathode surface is 25 MV/m. This induces a reduction of work function by the Schottky effect of 0.23 eV. Electrons are extracted from the cathode by photoemission using uv laser pulses with a Gaussian-like longitudinal profile of  $\sigma_{t,\text{laser}} = 4$  ps rms. They leave the diode through a 2 mm diameter hole in the anode and are accelerated in the rf cavity to energies of up to 6 MeV. The gun laser is a frequency-tripled Ti:sapphire amplifier and delivers Gaussian-like uv pulses of up to 900  $\mu\text{J}$ . The laser's central wavelength is tunable over a range of 260–282 nm with a spectral width of  $\Delta\lambda = 1$  nm. This corresponds to a variation of photon energy between 4.73 and 4.39 eV (Fig. 2). Important for accurate emittance characterization is a laser spot well defined in size and symmetry. A series of four aperture masks which can be positioned in the laser beam [7,10] provide well-defined flattoplike transverse intensity profiles on the cathode variable in diameter from 0.5 to 1.8 mm (full width). Electron beam charge was measured with a wall current monitor (WCM) and an integrating charge transformer (ICT) positioned at 1 and 2 m from the cathode, respectively. All measurements were performed at constant current density.

One of the two methods chosen here for measuring low charge emittance was the solenoid scan technique [11]. The solenoid located after the laser input port together with the scintillating screen at 1.2-m distance downstream

were used for this purpose. The pepper-pot technique [12] was the other method used for transverse emittance characterization. A tungsten pepper-pot mask (hole diameter 50  $\mu\text{m}$ , pitch 250  $\mu\text{m}$ , thickness 0.5 mm) followed by a yttrium aluminum garnet (YAG) screen at 0.43 m distance gives rise to the typical pattern of Fig. 3(b) from which emittance was calculated [5,13]. A thermoelectrically cooled sensitive camera (PCO SensiCam [14]) was used to image the YAG screen located in the emittance monitor. An acquisition time of 2 s (20 shots) was set for recording pepper-pot pictures at very low electron beam charge ( $<1$  pC) [see example in Fig. 3(b)]. For the solenoid scans, single shot acquisitions were sufficiently intense to record the electron beam size as a function of the applied solenoid current [Figs. 3(a) and 3(c)]. The complete scan over 20 A with about 100 data points took about 1–2 min. For the solenoid scan analysis, the transfer matrix of the solenoid was calculated by taking into account the measured field map of the solenoid. The best fit to the solenoid scan using the transfer matrix coefficient [Fig. 3(c)] gives then the emittance value. For the solenoid scan low electron bunch charge was used in order to avoid space-charge effects during solenoid focusing which would lead to a deterioration of emittance. In our experiment, an electron bunch charge of 0.2 pC was measured for the largest laser diameter (1.8 mm at full width) by help of the calibrated intensity signal observed on the YAG screens. Both emittance reconstruction methods used here are ultimately limited by the background and beam boundaries estimation leading to a precision of  $\pm 0.03$  mm  $\cdot$  mrad.

Figure 4 shows normalized intrinsic emittance measurements for a flat hand-polished, cleaned polycrystalline copper surface as a function of the laser spot size and for different laser wavelengths. As expected the intrinsic emittance decreases linearly with the laser spot size diameter. The shortest available laser wavelength (262 nm), commonly used for FEL gun lasers, yields an intrinsic emittance of  $0.17 \pm 0.03$  mm  $\cdot$  mrad for an emitting area diameter of 1 mm full width (i.e., 0.25 mm rms). Reducing the photon energy results in a reduction of emittance as it can be seen for 272 and 282 nm laser wavelengths. Indeed, the emittance decreases to  $0.1 \pm 0.03$  mm  $\cdot$  mrad for 1 mm laser spot size (full width) when using 282 nm laser pulses. The measured slopes can be well fitted by Eq. (1) if one assumes a work function of  $\Phi_0^{\text{Cu}} = 4.3$  eV (solid bold lines). This value is very close to the work function of atomically clean copper reported in

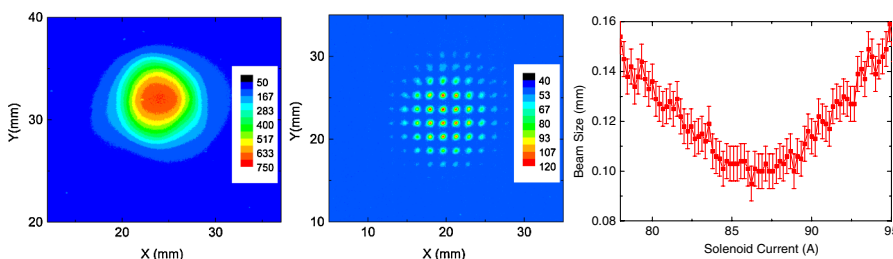


FIG. 3 (color online). (a) Electron beam shape at position of YAG crystal in emittance monitor (left). (b) Pepper-pot image for emittance reconstruction 0.23 mm  $\cdot$  mrad (middle). (c) Electron beam size in function of solenoid current 0.24 mm  $\cdot$  mrad (right). ( $Q < 1$  pC; 261 nm, Cu inset.)

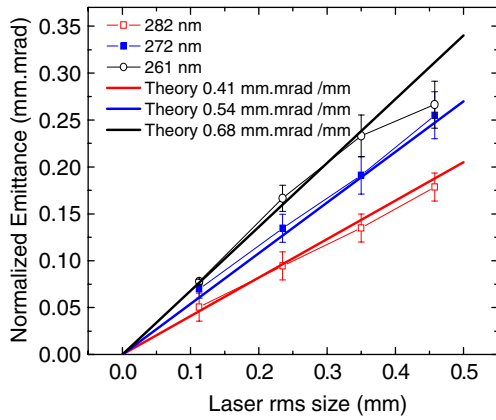


FIG. 4 (color online). Normalized projected emittance versus laser spot size for 3 different wavelengths on copper. ( $Q < 1$  pC; solenoid scan method, Cu inset). Theory corresponds to Eq. (1) assuming  $\Phi_{\text{Cu}} = 4.3$  eV (thermal effects not included).

literature (4.31 eV) [9]. The measured intrinsic emittance per millimeter for copper evolves from 0.68 mm · mrad/mm for a laser wavelength of  $\lambda_c = 262$  nm to 0.41 mm · mrad/mm for  $\lambda_c = 282$  nm. This is in good agreement with theoretical expectations. Error bars in Fig. 4 indicate the span of emittance reconstruction uncertainty when estimating the background level and/or the beam boundary. In our calculations no field enhancement due to surface roughness has been assumed and the effective surface field used here is the applied field of 25 MV/m. The Schottky effect leads then to an effective work function of  $\Phi_{\text{eff}} = 4.07$  eV which means that the initial kinetic energy of photoelectrons is about  $E_{\text{kin}} = 0.33$  eV ( $E_{\text{kin}} = \Phi_{\text{eff}} - \hbar\omega$ ) at 282 nm compared to  $E_{\text{kin}} = 0.66$  eV at 262 nm, neglecting the thermal energy of electrons. To reduce the intrinsic emittance even further one would need a longer laser wavelength to exactly match the effective work function. Then the intrinsic emittance is dominated by the thermal energy of the electrons and by other phenomena such as transient effects due to laser heating on the cathode and the energy spread of the laser pulse.

Figure 5 represents the projected normalized emittance in units of mm · mrad per millimeter of laser spot size (rms). Good agreement between the two measurement techniques (pepper-pot and solenoid scan) is obtained. With those two methods we have systematically explored the intrinsic emittance in units of mm · mrad per millimeter of laser spot size (rms) for different materials and for different laser wavelengths. Measurements performed on metallic cathodes (Cu, Mo, Nb [(110) single crystal] and Al) are depicted in Fig. 6 together with theoretical predictions for different work functions (solid lines) according to Eq. (1). Compared to copper, molybdenum presents similar emittance values suggesting an almost identical work function which is in agreement with literature [15]. Higher intrinsic emittance values are expected for materials with a smaller work function than copper such as aluminum

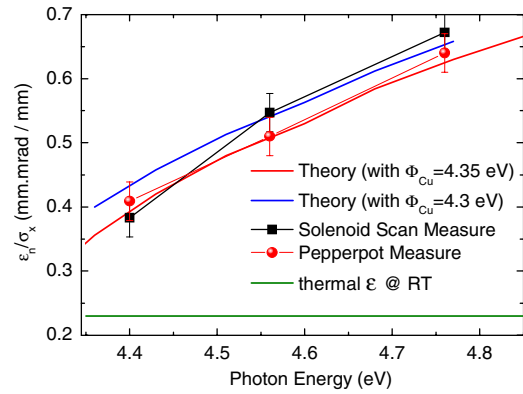


FIG. 5 (color online). Intrinsic emittance in unit of mm · mrad per mm laser spot size (rms) measured with pepper-pot and solenoid scan ( $Q < 1$  pC; copper inset); theory corresponds to Eq. (1) (thermal effects not included). Also shown is the thermal emittance at room temperature (300 K).

or niobium. This is confirmed on Fig. 6 where best fits to Eq. (1) are obtained for  $\Phi_0^{\text{Al}} = 3.9$  eV for aluminum and  $\Phi_0^{\text{Nb}} = 4.1$  eV for niobium (Fig. 6). These values are compatible to work functions reported in the literature [16,17] (4.2 eV for Al, 4.3 eV for Nb) taking into account surface contamination.

While the lowest uv photon energy provided by our laser system (4.4 eV, Fig. 2) matches almost exactly the work functions of Cu and Mo ( $\Phi_0^{\text{Cu}} \sim 4.3$  eV,  $\Phi_0^{\text{Mo}} \sim 4.35$  eV), a significant energy mismatch is present for Al and Nb. This leads to an increase of uncorrelated kinetic energy of the electrons released from the cathode into the vacuum. For a given laser wavelength, we have measured an emittance increase of 50% for Al and 30% for Nb in comparison to intrinsic emittance of copper. Naturally, an extension of the laser wavelength tuning range would again give the possibility to reduce emittance for those metals.

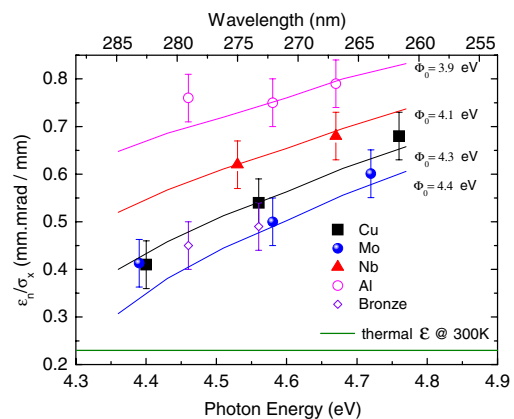


FIG. 6 (color online). Normalized intrinsic emittance/mm for different cathode materials at different laser photon energies with theoretical curves (solid lines) given by Eq. (1) for different work functions (thermal effects not included). Thermal emission at room temperature is displayed as well. The error bars result from deviation between pepper-pot and solenoid measurements.

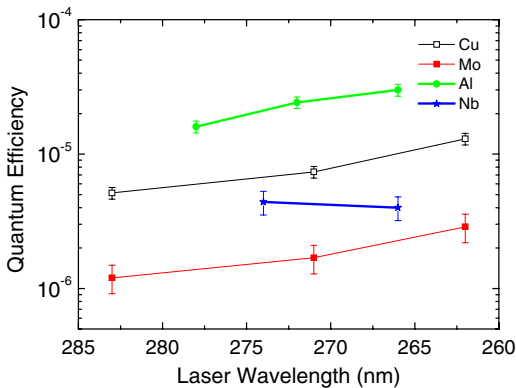


FIG. 7 (color online). Measured quantum efficiencies for Al, Mo, Nb, and Cu at different laser wavelengths (charge  $>20$  pC).

Matching the photon energy to the work function of the cathode material is expected to lower the quantum efficiency. Figure 7 shows the measured variation of QE with the laser for the above cited metals. The QE is determined by measuring the laser energy at the vacuum viewport entrance taking into account the losses from this position to the cathode ( $\sim 10\%$ ). For QE determination the laser energy was increased to measure charge above 20 pC with both the WCM and ICT at 1 and 2 m distance from the cathode, respectively. Observation of the same electron beam charge on both the WCM and the ICT insures that no charge is lost. Illumination of copper at  $\lambda = 262$  nm provides a quantum efficiency of  $1 \times 10^{-5}$  ( $\pm 1 \times 10^{-6}$ ) for a cathode surface field of 25 MV/m. Higher QE of up to  $2.0 \times 10^{-5}$  ( $\pm 2 \times 10^{-6}$ ) was found for aluminum while molybdenum shows almost an order of magnitude lower QE of  $3.0 \times 10^{-6}$  ( $\pm 0.6 \times 10^{-6}$ ) than Cu.

As expected from theory the quantum efficiency [6,8] drops for lower laser photon energies (i.e.,  $\lambda_c > 262$  nm). In fact, the change of quantum efficiency in dependence of laser wavelength was measured to vary by a factor of  $\leq 2.5$  over the explored wavelength range. Such QE at longer laser wavelength is still acceptable for electron guns and laser wavelength tuning offers therefore a great potential for low emittance electron sources. A comparison to a theory including thermal and transient effects important for electron extraction near the Fermi level goes beyond the scope of this Letter. In addition, other effects such as the work function variation of the different crystal faces on cathode surface, surface contamination, roughness, and heating effects should be taken into account to correctly interpret the measured curves [8]. The measured high QE at longer wavelengths is definitely advantageous for applications demanding low emittance. Such an electron source would be ideal for driving FELs operating in the so-called single-spike mode for providing (sub-) femtosecond x-ray pulses [18]. Such machines operate at significant lower charge ( $<20$  pC) than conventional FELs [1] but have more stringent requirements on emittance.

In conclusion, we studied the impact of laser wavelength tuning on the emittance and quantum efficiency of metallic cathodes and could demonstrate an efficient reduction of the intrinsic emittance. By adapting the laser photon energy to the effective work function of the cathode material, the projected emittance per mm laser spot size was reduced by 40% going from 0.68 to 0.41 mm · mrad/mm for a polycrystalline copper cathode while QE dropped only by 60%. Similar wavelength scans of intrinsic emittance were measured for other metallic cathodes (Mo, Al, Nb) and the trends are in agreement with the theory. With the state of the art laser technology presented here covering a wavelength range going from 262 to 282 nm, copper is the most promising candidate for FELs since it offers lowest intrinsic emittance (0.41 mm · mrad/mm at 282 nm) with a reasonable quantum efficiency ( $5 \times 10^{-6}$ ) at 25 MV/m surface gradient.

The authors acknowledge the support of M. Dach, M. Paraliiev, C. Gough, and I. Ivkovic. We are grateful to A.M. Valente-Feliciano from JLAB for providing the niobium samples and to Swiss National Science Foundation (Contract No. 200021\_122111/1).

- [1] Y. Ding *et al.*, *Phys. Rev. Lett.* **102**, 254801 (2009).
- [2] Y. Miltchev *et al.*, in *Proceedings of the 27th FEL Conference, Stanford, 2005* (JaCoW/eConf C0508213), <http://www.slac.stanford.edu/econf/C0508213/PAPERS/THPP042.PDF>.
- [3] B. D. Patterson *et al.*, *New J. Phys.* **12**, 035012 (2010).
- [4] B. D. Patterson, PSI, Switzerland Report No. 09-10, 2009.
- [5] R. Ganter *et al.*, in *Proceedings of the FEL09 Conference, Liverpool, U.K., 2009*, <http://accelconf.web.cern.ch/AccelConf/FEL2009/papers/tupc35.pdf>.
- [6] D. H. Dowell and J. F. Schmerge, *Phys. Rev. ST Accel. Beams* **12**, 074201 (2009).
- [7] C. P. Hauri *et al.*, in *Proceedings of the 27th FEL Conference*, <http://accelconf.web.cern.ch/AccelConf/FEL2009/papers/mopc63.pdf>.
- [8] K. L. Jensen *et al.*, *J. Appl. Phys.* **102**, 074902 (2007).
- [9] D. H. Dowell *et al.*, *Phys. Rev. ST Accel. Beams* **9**, 063502 (2006).
- [10] R. Akre *et al.*, *Phys. Rev. ST Accel. Beams* **11**, 030703 (2008).
- [11] M. Reiser, *Theory and Design of Charged Particle Beams* (John Wiley & Sons, New York, 1994).
- [12] S. J. Anderson *et al.*, *Phys. Rev. ST Accel. Beams* **5**, 014201 (2002).
- [13] <http://amas.web.psi.ch/tools/XanaROOT/>.
- [14] <http://www.pco.de/sensitive-cameras/>.
- [15] D. E. Eastman, *Phys. Rev. B* **2**, 1 (1970).
- [16] *Handbook of Chemistry and Physics*, edited by D. R. Lide (CRC Press/Taylor & Francis, Boca Raton, FL, 2010).
- [17] B. J. Hopkins and M. Ibrahim, *Vacuum* **23**, 135 (1973).
- [18] S. Reiche *et al.*, in *Proceedings of the FEL09 Conference, Liverpool, U.K., 2009*, <http://accelconf.web.cern.ch/accelconf/FEL2009/papers/mopc07.pdf>.